Transgenic Res (2013) 22:519–535
DOI 10.1007/s11248-012-9663-6

ORIGINAL PAPER

A plant derived multifunctional tool for nanobiotechnology based on *Tomato bushy stunt virus*

Simone Grasso · Chiara Lico · Francesca Imperatori · Luca Santi

Received: 27 July 2012 / Accepted: 24 September 2012 / Published online: 30 October 2012

Abstract Structure, size, physicochemical properties and production strategies make many plant viruses ideal protein based nanoscaffolds, nanocontainers and nanobuilding blocks expected to deliver a multitude of applications in different fields such as biomedicine, pharmaceutical chemistry, separation science, catalytic chemistry, crop pest control and biomaterials science. Functionalization of viral nanoparticles through modification by design of their external and internal surfaces is essential to fully exploit the potentiality of these objects. In the present paper we describe the development of a plant derived multifunctional tool for nanobiotechnology based on *Tomato bushy stunt virus.* We demonstrate the ability of this system to remarkably sustain genetic modifications and in vitro chemical derivatizations of its outer surface, which resulted in the successful display of large chimeric peptides fusions and small chemical molecules, respectively. Moreover, we have defined physicochemical conditions for viral swelling and reversible viral pore gating that we have successfully employed for foreign molecules loading and retention in the inner cavity of this plant virus nanoparticles system. Finally, a production and purification strategy from *Nicotiana benthamiana* plants has been addressed and optimized.

Keywords Viral nanoparticle · Nanovector · Nanobiotechnology · Plant made pharmaceutical · *Tomato bushy stunt virus*

Simone Grasso and Chiara Lico contributed equally to this work.

Electronic supplementary material The online version of this article (doi:10.1007/s11248-012-9663-6) contains supplementary material, which is available to authorized users.

S. Grasso
University Campus Bio-Medico, Via Alvaro del Portillo 21, 00128 Rome, Italy

C. Lico
UTBIORAD-FARM, ENEA C. R. Casaccia, Via Anguillarese 301, 00123 S. Maria di Galeria, Rome, Italy

F. Imperatori · L. Santi (✉)
Department of Agriculture, Forests, Nature and Energy (DAFNE), Università della Tuscia, Via San Camillo de Lellis snc, 01100 Viterbo, Italy
e-mail: luca.santi@unitus.it

Introduction

The natural feature of some biological molecules to form well defined super molecular structures has been increasingly exploited as a valuable technology. In particular, the peculiarity of viruses to self assemble during replication and infection into protein based nanoparticles has received much attention since the early days of nanotechnology. Many examples include non-enveloped virus particles composed of the multimerization of a single coat protein (CP) that precisely assembles into structural architectures. Bacteriophages (Bar et al. 2008; Newton-Northup et al. 2009), animal

(Murata et al. 2009; Santi et al. 2008) and plant viruses (Gonzalez et al. 2009; Lico et al. 2009) have been all investigated for their use as tools in a broad range of applied fields, extending from biomedicine to materials science (Lewis et al. 2006; Nam et al. 2006). Viral nanoparticles (VNPs) have a size particularly suitable for nanoscale applications and can offer several advantages over non biological nanoparticles: they are homogeneous in size (monodispersion), they bear an intrinsic robustness being at the same time naturally biodegradable and they have a large surface area to mass ratio and a defined, repetitive and symmetric macromolecular organization.

A common requirement for advanced nanoscale applications is to fully take advantage of multivalency and payload containment and transport. Also in this respect VNPs present several benefits. Viral capsids have been designed by nature to carry nucleic acids and in some cases non-structural proteins in their interior cavity, where they are confined and protected during transfer throughout extremely different environments. Moreover, many viruses are able to achieve tropism to certain organs and cell types, often as a result of characteristics related to the specific affinity of exposed portions of their CP to target cell receptors (Ashley et al. 2011; Singh 2009). Different strategies for the modification of VNPs' outer and inner surfaces as well as for entrapment of molecules in their inside have been addressed in order to thoroughly take advantage of the described virus properties (Grasso and Santi 2010). The growing knowledge of the structure of viruses at high resolution level, together with the ease of manipulation of viral genomes, has allowed the development of a vast plethora of chimeric virus nanoparticles (CVNPs). Via genetic fusion of heterologous coding sequences (CDSs) to defined positions of the CP gene (*cp*), peptides with the most diverse biological functions have been displayed on VNPs outer surface (Gleiter and Lilie 2001; Hajitou et al. 2006; McCormick et al. 2006; van Houten et al. 2006) and, in a reduced number of cases, on their inner surface (Beterams et al. 2000). As an alternative or in combination with genetic modification, bioconjugation has been broadly addressed to expose not only peptides but also entire complex proteins, organic molecules and polymers such as nucleic acids and polyethylene glycol (Raja et al. 2003; Smith et al. 2006; Strable et al. 2004). The amine functional group of lysine is a common target for conjugation through *N*-hydroxysuccinimide (NHS) ester based chemistry (Steinmetz et al. 2010; Wang et al. 2002). Entrapment into VNPs has mainly been achieved in vitro, in presence of high concentrations of foreign molecules, by disassembly/reassembly of capsids (Chen et al. 2006; Comellas-Aragones et al. 2007; Ren et al. 2006) or by the reversible opening of viral gated pores (Douglas and Young 1998; Loo et al. 2008). Both methods require controlled tuning of physicochemical conditions such as temperature, pH and concentration of metal ions.

In particular, also plant viruses have received a great deal of interest as potential source of VNPs. Spherical as well as rod shape particles have been manipulated to develop novel nanotechnological tools for drug delivery, bioimaging, biomaterials and nanostructured electronic devices (Fowler et al. 2001; Lewis et al. 2006; Nam et al. 2006; Prasuhn et al. 2007; Ren et al. 2007). The vast majority of plant viruses has a small, single stranded, positive-sense RNA genome, that can be simply retro-transcribed into a cDNA infectious clone. Their limited genome size, together with the precise knowledge of their sequence, offers the possibility of de novo synthesis of their entire genome, making natural bioblocks even easier to obtain and use for the construction of new systems. The vast majority of plant viruses is non-infectious toward other organisms and therefore their use in biomedicine presents no biological hazard. Moreover, plants have been extensively reported as excellent bioreactor systems. They are safe, cost-effective and highly scalable. VNPs production in plants and their subsequent purification is simple, efficient, high yielding and quick (Chen and Lai 2013; Lai and Chen 2012; Santi et al. 2006; Scholthof et al. 1996).

Tomato bushy stunt virus (TBSV), the prototype member of the *Tombusviridae* family, has a monopartite, single stranded, positive-sense RNA genome of nearly 4,8 kb that contains five open reading frames (ORF) between a 5′-uncapped untranslated region (UTR) and a non-polyadenilated 3′ UTR. The third 5′-proximal ORF encodes the unique viral CP, p41, which is translated from a subgenomic *m*RNA into a product of ~41 kDa (White and Nagy 2004). The ternary structure of the CP subunit is defined by three separate domains: the RNA binding domain (R) formed by the N-terminal residues, the shell domain (S) and the C-terminal protruding (P) domain. The viral capsid is made of 180 copies of the CP subunit that self

assembles into particles of ~30 nm in diameter with a spherical shape originated from a $T = 3$ icosahedral symmetry. In the context of this quaternary arrangement the CP R domain is placed at the interior of the virus particle, while the C-terminal P domain is exposed on the external surface (Harrison et al. 1978; Olson et al. 1983).

In this study we present the development of an efficient and versatile system for VNPs production in *Nicotiana benthamiana* based on the TBSV pepper isolate (Szittya et al. 2000). In particular, we report the construction of a vector which allows the generation of genetic fusion at the C-terminal end of the TBSV CP, resulting in the display of peptides outside the viral protein capsid. We tested the system by progressively fusing 4 CDSs of commonly used protein tags, one after the other in a modular fashion. We proved at different levels that all the obtained CVNPs were able to retain infectivity and proper structural assembly, reaching with the longest chimera the correct exposure of 56 additional amino acids. We used one of the chimera to address bioconjugation of biotin on genetically introduced lysine residues and we tuned an experimental method for virus reversal permeability, setting the ground for foreign molecules entrapment. Finally, we have optimized a purification protocol, determined yield and developed production standards.

Materials and methods

Genetic engineering

The construction of TBSV chimeras displaying specific tag peptides in fusion with the viral CP was achieved by standard recombinant DNA technologies (Sambrook and Russell 2001). All the first steps of genetic engineering were performed on a subclone obtained by *NotI*/*NcoI* digestion of the TBSV–P plasmid (Szittya et al. 2000) (Fig. 1a) followed by the introduction of the generated fragment, encoding for the C-terminal region of the CP, into the pBluescript SK (+) vector. A multi-cloning site (MCS) was inserted first by transforming the *cp* stop codon (Fig. 1b) into a *ClaI* restriction recognition site, which has then been used for vector digestion and ligation with the compatible in vitro annealed oligonucleotides (MCS-For, MCS-Rev; Online Resource 1) harboring the *ApaI* and *PacI* sites. The substitution of the *amber* stop codon with the *ClaI* sequence was obtained using the QuikChange® II-E Site-Directed Mutagenesis Kit (Stratagene) by means of two primers presenting the desired mutation (TBSV Mut-For, TBSV Mut-Rev; Online Resource 1). At this stage, the modified 3′-terminal *cp* sequence was moved back into the TBSV genome context upon *NotI*/*NcoI* digestion, generating the TBSV–vector (the modified region is detailed in Fig. 1c). The Flag CDS (corresponding to the DYKDDDDK peptide, Chiang and Roeder 1993), designed using preferential codon bias of *N. benthamiana* and spaced from the last *cp* nucleotide by a GGPGGGG linker CDS, was the first tag introduced in the polylinker of the previously generated vector. The vector was digested *ApaI*/*PacI* and ligated with the in vitro annealed Flag encoding oligonucleotides (Flag-For, Flag-Rev; Online Resource 1), owning compatible protruding ends, thus generating the TBSV–Flag (Fig. 1d). Subsequently, the TBSV–Flag construct was digested *ApaI*/*PacI* and the compatible in vitro annealed cMyc–Flag fusion CDS (cMyc-For, cMyc-Rev; Online Resource 1) (Kawarasaki et al. 2003) was introduced, producing the TBSV–cMyc (bearing the EQKLISEEDL cMyc peptide, derived from the c-myc proto-oncogene product, in addition to the Flag sequence; Fig. 1e). Next, the TBSV–cMyc construct was opened at *ApaI* site and the compatible in vitro annealed HA oligonucleotides (HA-For, HA-Rev; Online Resource 1) (coding for the YPYDVPDYA peptide, derived from the influenza Hemagglutinin, Laize et al. 1997) were ligated generating, upon correct orientation colony screening, the TBSV–HA (Fig. 1f). The same strategy was then used to clone the V5 fragment (corresponding to the GKPIPNPLLG LDST epitope, derived from the P/V proteins of the paramyxovirus simian virus 5, SV5; Kolodziej et al. 2009) using a synthetic oligonucleotides pair (V5-For, V5-Rev; Online Resource 1) creating the TBSV–V5 (Fig. 1g). In all cases, to separate each tag module from the others, GPG linker CDSs have been introduced by design into the encoding tag oligonucleotides. As for the Flag CDS, all tags CDSs were in silico optimized for *N. benthamiana* codon usage. To produce an alternative approach to viral in vitro transcription for infection, the T7 promoter of the original TBSV–P construct was replaced with the *Cauliflower mosaic virus* (CaMV) 35S promoter (Odell et al. 1985). The CaMV 35S sequence was amplified by PCR using the pPVX204 expression vector (Baulcombe et al. 1995)

as a template and a pair of specific primers: the TBSV–35S–For primer (Online Resource 1), owning a 5′ *BamHI* extension, and the TBSV–35S–Rev primer (Online Resource 1). The 5′ TBSV genome context was amplified by PCR using a forward primer (TBSV-5′ context-For; Online Resource 1) covering the authentic 5′ end of TBSV genome (Hearne et al. 1990) and a reverse primer (TBSV-5′ context-Rev; Online Resource 1) with 5′ *AgeI* extension. Next, both PCR products properly restricted were included in a three fragments ligation with the TBSV–cMyc construct, previously digested *BamHI*/*AgeI*, generating the 35S–TBSV–cMyc construct (Fig. 1h). The *Agrobacterium tumefaciens* nopaline synthase (NOS) termination sequence (Depicker et al. 1982) was introduced downstream of the 3′ viral end. Also in this case, the NOS sequence was amplified by PCR using the pPVX204 expression vector as a template and two specific primers: the forward primer (PCR–NOS–For; Online Resource 1) with a 5′ *XmaI* extension and the reverse primer (PCR–NOS–Rev; Online Resource 1) with a 5′ *SacI* extension. Also the *Hepatitis delta virus* (HDV) antigenomic ribozyme (HRz) sequence was introduced (Chowrira et al. 1994) (the fragment, owning *XmaI* compatible ends, was generated by in vitro annealing of two complementary oligonucleotides; HRz–For, HRz–Rev; Online Resource 1). Subsequently, the 35S–TBSV–cMyc construct and the NOS fragment were *XmaI*/*SacI* digested and included in a three fragments ligation with the HRz sequence. The resulting constructs were screened for the presence of NOS (for the 35S–TBSV–cMyc.NOS vector; Fig. 1i) or of both fragments in the correct orientation (for the 35S–TBSV–cMyc.riboNOS vector; Fig. 1j). All clones were verified by sequencing (BMR Genomics) with specific primers (TBSV–1For, TBSV–2Back and ScreenNOS-Rev; Online Resource 1). All primers and oligonucleotides used in this work were synthesized at MWG-Biotech.

Plant infection

Six to eight weeks old *N. benthamiana* plants, grown in controlled conditions (24 °C, 16 h light/8 h dark), were inoculated with different TBSV constructs as described below.

cDNA templates of TBSV–P (that in vivo produces TBSV wild-type particles, TBSV–wt), TBSV–Flag, –cMyc, –HA and –V5 constructs were linearized by *Xma*I digestion. One μg of completely linearized cDNA was used for in vitro transcription following the manufacturer's instructions (MEGAscript® T7 High Yield Transcription kit, Ambion Applied Biosystems). Integrity of the infectious transcribed RNA was verified by TBE agarose gel electrophoresis.

Plants were mechanically inoculated abrading the adaxial side of 2 leaves per plant using the TBSV infectious RNAs or the TBSV in planta expression vectors mixed with carborundum (silicon carbide) powder (VWR International). For each leaf inoculation, approximately 2–3 μg of the in vitro transcribed RNA were diluted in ultrapure sterile water up to a volume of 50 μl.

Plasmidic DNA of 35S–TBSV–cMyc, –cMyc.NOS and –cMyc.riboNOS constructs was extracted using the Plasmid Maxi kit (QIAGEN). Primary-infected plants were obtained by direct inoculation with cDNA vector on 2 healthy leaves per plant (30 μg for each leaf), as previously described; only the 35S–TBSV–cMyc cDNA was linearized by *Xma*I digestion before infection.

Reinfections were performed using saps from infected leaves. Briefly, a raw leaf sap was prepared by homogenizing the symptomatic systemic tissue of an infected plant in Phosphate Buffered Saline (1× PBS: 151 mM NaCl, 8,4 mM $Na_2HPO_4 \times 12\ H_2O$, 1,86 mM $NaH_2PO_4 \times H_2O$).

VNPs purification

Virus particles were purified following the protocol of Burgyan and Russo (1998) with some modifications. Infected leaves were collected 7–9 days post-infection (dpi) and ground to a fine powder. Plant material was homogenized with 3 ml/g of 50 mM sodium acetate, pH 5.3, supplemented with 1 % ascorbic acid and a cocktail of protease inhibitors (P9599, Sigma) and the obtained solution was clarified by low-speed centrifugation (8,000×*g* for 15 min at 4 °C). During homogenization plant material lowered the pH of the extract and therefore NaOH was added to reach pH 5.0. The supernatant was then ultra-centrifuged for 1 h at 90,000×*g* at 4 °C. The obtained pellet was resuspended in 50 mM sodium acetate, pH 5.3. Quality of the preparations was verified by a silver stained 13.5 % SDS–PAGE. Virus concentration was evaluated using the Bradford micro-assay procedure

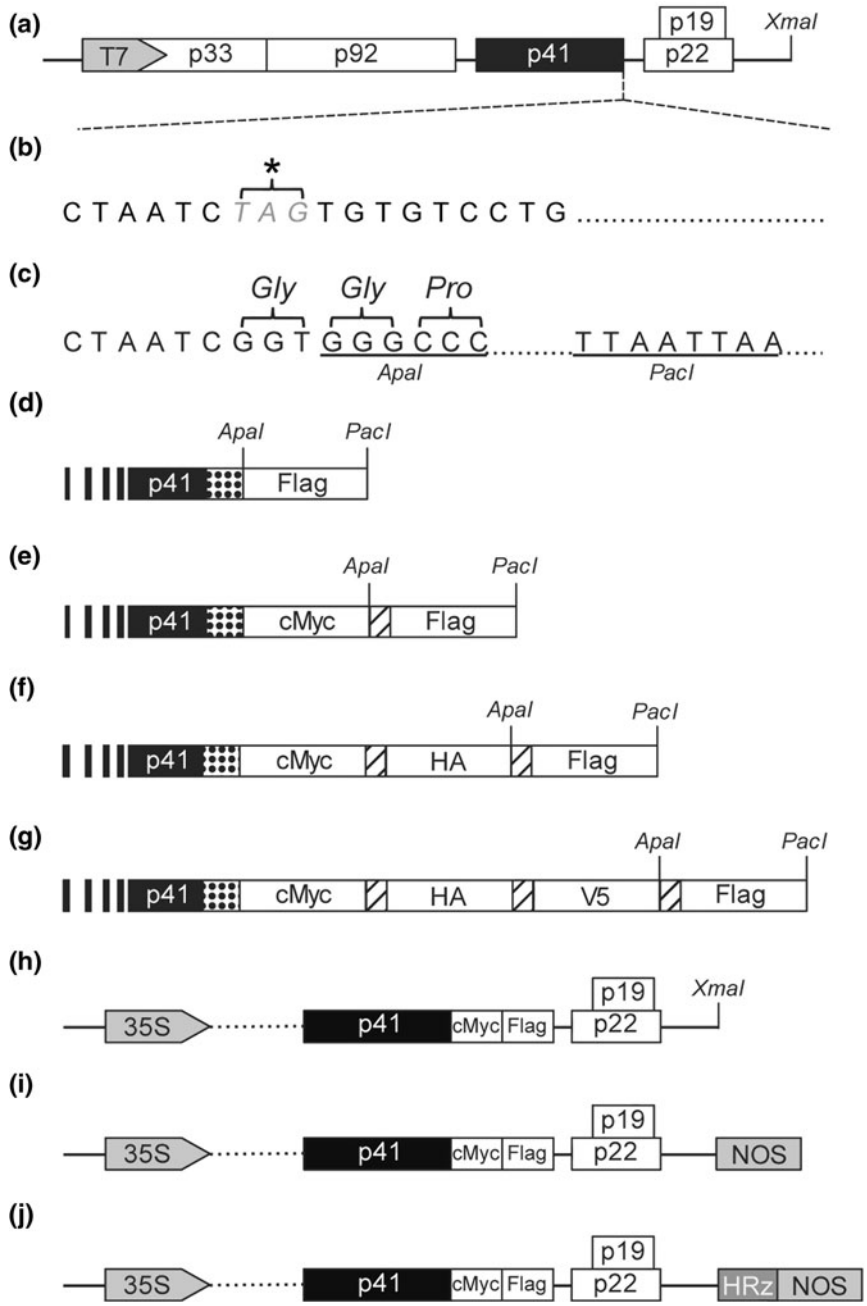

Fig. 1 Schematic representation of TBSV cDNA constructs. **a** Genome organization of TBSV–P plasmid. The 5 ORFs encoding the respective proteins with their molecular masses (in kDa) are represented as *boxes*: p33 and p92 (RNA-dependent RNA polymerase), p41 (CP), p22 (movement protein), p19 (silencing inhibitor). **b** Sequence detail of the original and **c** of the genetically engineered CP stop codon (*asterisk*) region (TBSV–vector). The first amino acids of the GGPGGGG linker are reported. The *underlined* sequences represent the restriction enzyme sites used to clone the peptides of interest. As simplification, it is illustrated only the 3′-*cp* engineered region of the **d** TBSV–Flag, **e** TBSV–cMyc, **f** TBSV–HA, **g** TBSV–V5 constructs. The *dotted boxes* represent the GGPGGGG spacer and the *striped boxes* the GPG amino acid linker. **h**–**j** Genome organization of 3 TBSV–cMyc expression vectors based on the *CaMV* 35S promoter and the *A. tumefaciens* NOS terminator **h** 35S–TBSV–cMyc, **i** 35S–TBSV–cMyc.NOS, **j** 35S–TBSV–cMyc.riboNOS. The *dotted line* schematically represents the whole genomic sequence between the first 5′ TBSV nucleotide and the p41 ORF. The HDV antigenomic ribozyme sequence is indicated as "HRz" named *box*

(Bio-Rad) and confirmed through an SDS–PAGE followed by a Coomassie Brilliant Blue staining.

Electron microscopy

Purified virus particles were collected on carbon/formvar film coated 400 mesh copper grids (Electron Microscopy Sciences) and stained with 2 % (w/v) uranyl acetate aqueous solution. Grids were then analyzed by using a transmission electron microscope JEM 1200 EXII (Jeol) and images were acquired through a CCD Camera SIS Veleta (Olympus) at the Interdipartimental Center of Electronic Microscopy (University of Tuscia).

Sucrose gradient

A discontinuous sucrose density gradient was prepared by layering successive decreasing concentrations of sucrose solutions. Briefly, 2 ml each of 60, 50, 40, 30, 20 and 10 % (w/v) sucrose dissolved in PBS were poured into ultracentrifuge tubes and a volume of 200 µl of the crude extract was loaded on top of the gradient. The analytical separation occurred by ultracentrifugation at 90,000×*g* for 2 h at 4 °C. Eleven fractions were collected from the top to the bottom of the tube. One hundred µl of each sample were finally analyzed by ELISA using a specific anti-Flag antibody or the DSMZ kit (AS-0098), which employs specific antibodies for the TBSV–wt detection.

SDS–PAGE analysis and immunoassays

Plant purified virus particles were mixed with standard Laemmli Loading Buffer supplemented with EDTA to a final concentration of 5 mM, denatured by heating for 1 min at 60 °C and resolved on a 13.5 % SDS–PAGE (Laemmli 1970). Proteins were electrophoretically transferred to a polyvinylidene difluoride (PVDF) membrane (Millipore) using a semidry blotting apparatus (TE70X semi-dry transfer unit, Hoefer). Subsequently, after blocking and washings, the membrane was probed with the specific primary antibody followed by incubation with the proper secondary horseradish peroxidase (HRP)-conjugated antibody. Signal detection was obtained by enhanced chemiluminescence (Immobilon Western Chemiluminescent HRP Substrate, Millipore).

Equal amounts of total soluble proteins (about 20 µg for each well) or plant purified virus particles were also analyzed by ELISA. Briefly, ELISA Maxisorp multiwell plates (NUNC) were coated with 100 µl of sample per well. Subsequently, 100 µl of the specific primary antibodies were added to each well. After incubation and washing the plates were probed with the proper secondary HRP-conjugated antibodies. Colorimetric reaction was developed using 2,2′-azino-bis(3-ethylbenzthiazoline-6 sulphonic acid) substrate (ABTS, KPL) and read at 405 nm on an automated ELISA reader (Sunrise, Tecan).

The primary antibodies and the respective dilutions used in this work were: mouse monoclonal M2 anti-Flag (1:4,000; F3165, Sigma), rabbit polyclonal anti-cMyc, -HA, or anti-V5 (1:2,000; PA1-22826, -86676, -32392 respectively, Thermo Scientific). For detection, anti-mouse IgG (NXA931, GE Healthcare) or sheep anti-rabbit IgG (PA1-84416, Thermo Scientific) HRP-conjugated secondary antibodies diluted 1:2,500 were used.

RNA extraction and RT-PCR analysis

Seven to nine dpi, total RNA was extracted from symptomatic inoculated and systemic leaves by using an RNeasy plant mini kit (QIAGEN) and RT-PCRs were performed by using 1 µg of extracted RNA for each sample and following the manufacturer's instructions (ProtoScript M-MuLV*Taq* RT-PCR kit, New England Biolabs). cDNA was synthesized by using random primers and PCR was carried out with TBSV specific primers (RT-PCR1For and TBSV–2back; Online Resource 1) to amplify the 3′ *cp* region (obtaining a 648 bp fragment in the wild-type context). The resulting fragments were finally purified and sequenced (BMR Genomics).

VNPs reversable swelling

Approximately 4 µg of purified TBSV–wt or –Flag particles were incubated in swelling buffer (0.1 M Tris, 50 mM EDTA, pH 8.5) or control buffer (0.1 M Tris, pH 5.5) at 4 °C for 2 h. To verify VNPs pore gating, ethidium bromide (EtBr) wad added during the incubation at a final concentration of 0.5 µg/ml. Samples were resolved by electrophoresis in 1 % agarose gel using an electrophoresis buffer containing 38 mM glycine and 5 mM Tris at pH 8.5. The gel was prepared in the same buffer and, after samples run, it was stained in swelling buffer with the addition of

EtBr at a final concentration of 0.5 μg/ml. Detection of virus particles was achieved by either visualization under UV light of the encapsidated RNA or Coomassie staining of the viral capsid protein.

RNAse protection assay

Four to six micrograms of TBSV–wt or –Flag particles were treated in swelling buffer or control buffer as described above. After 2 h 50 ng of ribonuclease A (New England Biolabs) were added to the reaction and the incubation was left at 4 °C for additional 30 min. Encapsidated RNA was extracted by the addition of an equal volume of a 1:1 phenol–chloroform solution (v/v) and SDS at a final concentration of 1 % (w/v). The mixture was agitated vigorously and then centrifuged to separate the two phases. The aqueous phase was recovered and the RNA was precipitated by the addition of 1/10 volume of 3 M sodium acetate and 3 volumes of ice cold ethanol. Finally, the RNA was sedimented by centrifugation and the pellet resuspended in RNAse free water. Integrity of the viral extracted RNA was analyzed by TBE 1 % agarose gel electrophoresis and visualized under UV light after EtBr staining.

Bioconjugation of biotin

In vitro biotinylation experiments were performed on TBSV–wt or –Flag particles following the EZ-Link® Micro NHS–polyethylene-oxide (PEO_4)-Biotinylation Kit (Thermo Scientific) manufacturer's instructions. Approximately 200 μg of VNPs were mixed with NHS–PEO_4 biotin reagent at tenfold molar excess and incubated 2 h in ice and then one additional hour at 4 °C. The excess non-reacted and hydrolyzed biotin reagent was removed by chromatography (Zeba™ Desalt Spin Column, 7000 MWCO; Thermo Scientific) and the purified samples (approximately 2 μg each) were analyzed by western blotting and ELISA using a streptavidin HRP-conjugated as probe (N100, Pierce).

Results

Genetic engineering

Several studies have demonstrated that the C-terminal portion of the TBSV CP is exposed on the exterior surface of the assembled virion (Harrison et al. 1978; Olson et al. 1983). Hence a TBSV based vector, for the generation of a peptide display system, was designed to contain the heterologous peptides CDSs genetically fused to the 3′ end of the viral *cp* gene. To this purpose, a MCS has been inserted in this region, through several subcloning steps, as described in the materials and methods section, involving as original source the TBSV–P plasmid (Szittya et al. 2000), which contains the whole viral genome sequence as cDNA downstream the T7 promoter (Fig. 1a). In essence, the thymine (T) and the guanine (G) contained in the native *cp amber* stop codon (TAG) (Fig. 1b) were converted into a specific *ClaI* recognition sequence (ATCGAT) by site directed mutagenesis. Subsequently, a MCS sequence, carrying the *ApaI* and *PacI* restriction sites, was inserted by means of in vitro annealed pair of oligonucleotides displaying 5′ and 3′ *ClaI* compatible ends, generating the TBSV–vector (Fig. 1c). Several chimeras were created by the insertion of different peptides CDSs into the TBSV–vector using the previously introduced unique restriction recognition sites. Four common tag peptides, named Flag (DYKDDDDK), cMyc (EQKLISEEDL), HA (YPYDVPDYA) and V5 (GKPIPNPLLGLDST), were chosen as candidates to test the potential of the TBSV to sustain the display of increasingly longer peptide sequences. As a result, four different constructs were generated by the progressive addition of the 4 tags CDSs assembled together one after the other in a modular fashion. Tag peptides encoding oligonucleotides were designed using *N. benthamiana* preferential codon bias and were subcloned, upon in vitro annealing, to generate the 4 different engineered viral constructs encoding chimeric CPs progressively increasing in length: TBSV–Flag (Fig. 1d), TBSV–cMyc (including also Flag peptide CDS, Fig. 1e), TBSV–HA (including also Flag and cMyc peptides CDSs, Fig. 1f) and TBSV–V5 (including also Flag, cMyc and HA peptides CDSs, Fig. 1g), respectively resulting in extensions of 15, 28, 40 and 56 amino acids compared to the wild-type CP. The TBSV–vector is devoid of the original stop codon thus, during the in silico design process, a stop codon was introduced at the 3′ end of the Flag CDS, which represents the most distal module in every construct.

Moreover, the 5′ end of each fusion peptide CDS was in silico designed in order to generate, upon genetic fusion, a GGPGGGG linker peptide between

the CP and the first tag module, and a GPG linker peptide between each of the subsequent adjacent modules. In fact, GPG based spacers were adopted to provide flexibility between the CP and the exogenous fragment, to avoid undesirable secondary structures that might interfere with chimeric CP folding and chimeric virus assembly, and to foster spatial and functional independence of multiple tag peptides.

To produce an alternative approach for the plant infection, which is normally obtained through the inoculation of infectious in vitro transcribed RNA, an in vivo transcription model strategy was designed. Using the TBSV–cMyc construct as a template, the CaMV 35S promoter sequence was introduced in place of the original T7 promoter, thus generating the 35S–TBSV–cMyc (Fig. 1h). Two additional constructs, both harbouring the cDNA of the TBSV–cMyc under the control of the CaMV 35S promoter, have been then assembled modifying the 3′ end context downstream the virus sequence: the 35S–TBSV–cMyc.NOS (Fig. 1i) additionally contains the termination sequence of the *nos* gene of *A. tumefaciens* and the 35S–TBSV–cMyc.riboNOS (Fig. 1j) has the HRz sequence introduced between the 3′ end of the genome and the NOS sequence. This particular ribozyme element, already employed by Scholthof (1999), when properly inserted is capable, through auto catalytic activity, to generate 3′ RNA terminal sequences identical to those of the TBSV genome, eliminating regions derived from nuclear transcription and normally not present on the infectious viral RNAs, such as the poly-adenylation signals.

Infectivity and in vivo assembly of VNPs

TBSV–P (that in vivo produces TBSV–wt particles), –Flag, –cMyc, –HA and –V5 vectors were linearized by digestion with *XmaI* restriction enzyme, purified and used for the in vitro transcription of infectious RNAs. TBSV RNAs were used to inoculate 6–8 weeks old *N. benthamiana* plants by gently rubbing the surfaces of 2 leaves per plant with silicon carbide and distributing on each leaf approximately 2–3 µg of RNAs. The symptomatology was constantly monitored and documented by photo capturing (data not shown). Plants inoculated with infectious TBSV RNAs showed the characteristic chlorotic local lesions onto inoculated leaves at 2–3 dpi. At 5–7 dpi symptoms appeared systemically showing mottling, severe distortion and stunting of the leaves. Necrosis of the apical shoots and finally the death of the plant occurred between 11 and 14 dpi. Differences between plants inoculated with infectious TBSV–wt or –chimeras RNAs, in terms of symptoms progression and severity, were not observed.

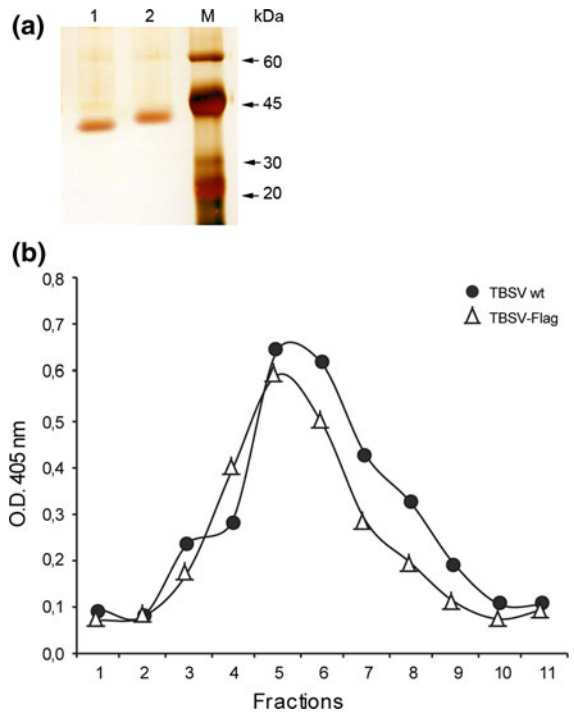

Fig. 2 Evaluation of particles purification and assembly. **a** Silver stained SDS–PAGE of purified TBSV–wt (1 µg, *lane 1*) and TBSV–Flag (1 µg, *lane 2*). Standards molecular weights are shown on the *right* of the *figure*. **b** Sucrose gradient sedimentation analysis. Crude extracts from TBSV–wt and –Flag *N. benthamiana* infected plants were analyzed on a 10–60 % sucrose gradient; 11 fractions were collected from the *top* to the *bottom*. The presence of TBSV particles in the collected fractions was determined by ELISA using anti-TBSV–wt CP (*filled circle*) and anti-Flag peptide (*empty triangle*) antibodies

Leaves showing systemic infection were harvested at 7–9 dpi and virus particles were purified following the protocol of Burgyan and Russo (1998) with some modifications. The recovery was about 300 µg of VNPs per gram of fresh leaf tissue. The quality of each purification was verified by a silver stained SDS–PAGE (Fig. 2a).

To verify the proper assembly of TBSV–chimeras, crude extracts of symptomatic TBSV–wt or –Flag infected leaves were subjected to sucrose sedimentation analysis. Eleven fractions were collected from the

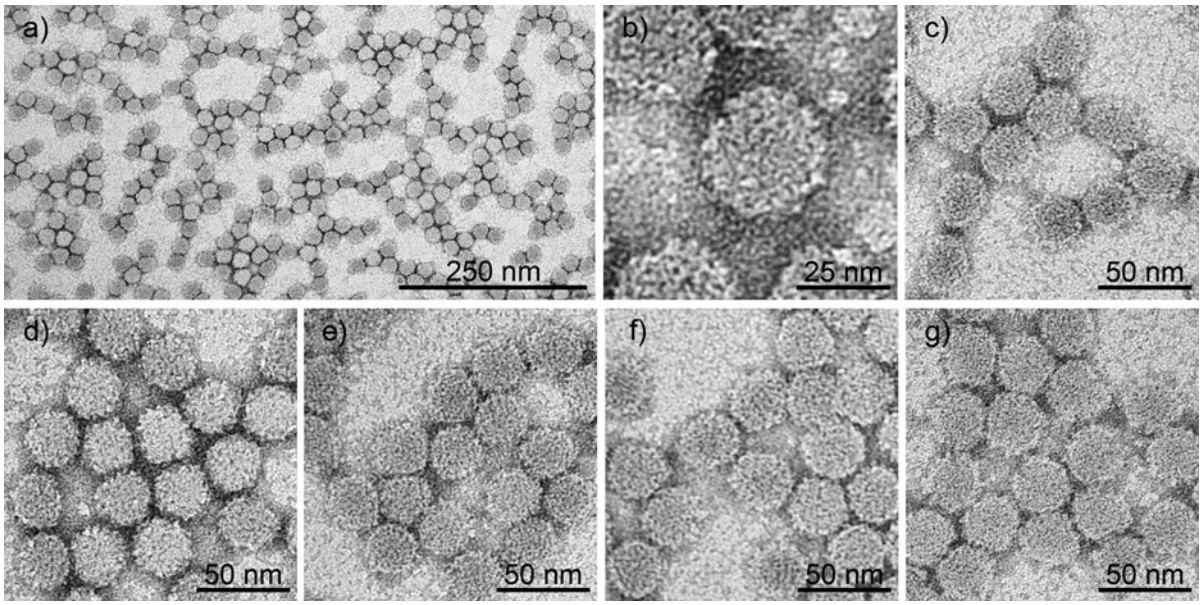

Fig. 3 Visualization by negative staining and high resolution electron microscopy of purified TBSV–wt and –chimeras particles. **a–c** TBSV–wt displayed at different magnifications, **d** TBSV–Flag, **e** TBSV–cMyc, **f** TBSV–HA, **g** TBSV–V5

sucrose gradient and further analyzed by ELISA with specific antibodies against the viral CP or the Flag tag. The sedimentation profiles of TBSV–wt and –Flag crude extracts were similar (Fig. 2b).

To obtain direct evidence of TBSV nanoparticles formation, purified TBSV–wt and –chimeras particles were subjected to transmission electron microscopy analysis. For all samples, VNPs with a diameter of about 30 nm were observed (Fig. 3).

CVNPs characterization

The leaves of primary infected plants showing systemic symptoms were harvested at 7–9 dpi and the genetic stability of the chimeric *cp* genes was verified by RT-PCR and sequencing. The mobility shift of PCR fragments on agarose gel (Fig. 4a) represents the different length of the constructs at genomic level, and the sequencing of the bands confirmed the presence of the correct heterologous sequences. To further characterize the TBSV constructs, purified TBSV–wt and all TBSV–chimeras were subjected to denaturation. Different protocols were tested to avoid protein aggregates (data not shown), finding as the best parameters heating at 60 °C for 1 min in the presence of EDTA at a final concentration of 5 mM. A quantity of 1 μg of purified denatured proteins for each construct was resolved by 13.5 % silver stained SDS–PAGE (Fig. 4b, upper panel). For all chimeric CPs, differences observed in the mobility through the acrylamide gel confirmed their expected sizes. Since all CVNPs displayed the Flag tag as part of the CP fusion peptide, the same samples were analyzed by western blotting using the anti-Flag specific antibody (Fig. 4b, lower panel). Results showed the presence of the Flag tag in all the fusion assemblies, confirming the expected molecular weight of the different chimeric CPs (Fig. 4b, lower panel). Finally, the absence of degradation products indicated that proteins were stable under purification and storage conditions. ELISA analysis was performed with antibodies specific to each single tag to assess the correct exposure of the fusion peptides on the surface of assembled CVNPs (Fig. 4c). A total protein raw extract was prepared from the infected tissue of plants inoculated with all the different constructs. Normalized extracts were evaluated with ELISA and a crude extract of a not-infected *N. benthamiana* plant was used as a negative control. Specific binding of the anti-tag antibodies directed against the chimeras was observed. Anti-Flag, -cMyc, -HA and -V5 antibodies were able to recognize the corresponding tag peptide (Fig. 4c), expressed as C-terminal fusion of the CP, demonstrating the correct

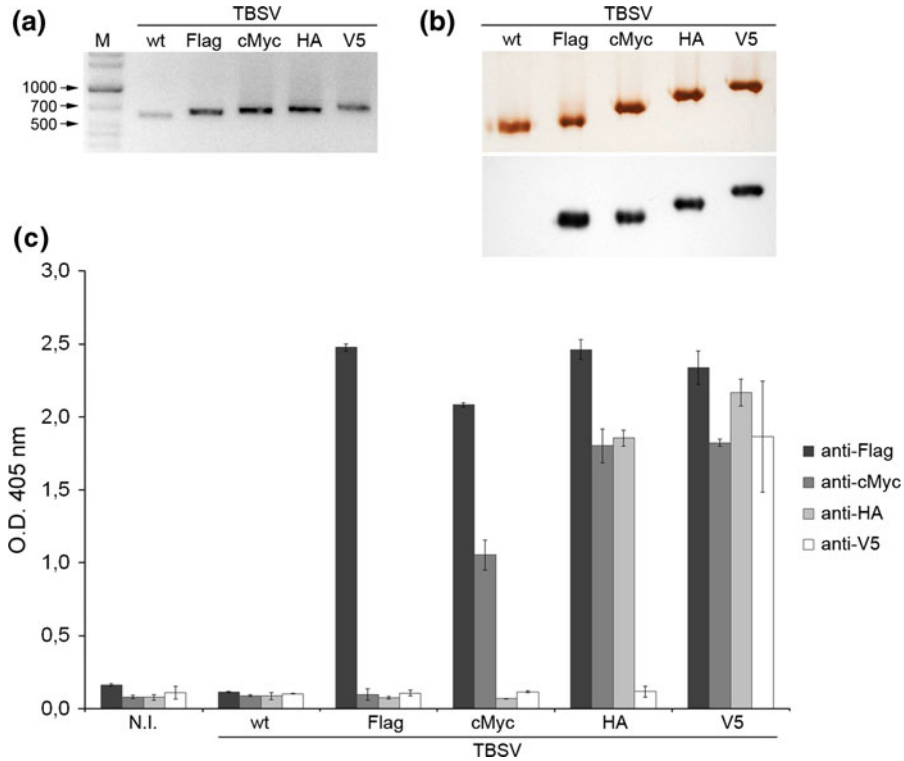

Fig. 4 Molecular characterization of TBSV vectors. **a** Evaluation of the presence of the heterologous sequences at genomic level. Agarose gel electrophoresis of RT-PCR covering the 3′ *cp* end of the TBSV–wt (fragment of 648 bp) and of all TBSV–chimeras. **b** SDS–PAGE analysis of denatured particles. TBSV–wt and all the TBSV–chimeras CPs were analyzed by silver staining (*upper panel*) and western blot (*lower panel*) using an anti-Flag antibody. **c** ELISA analysis of properly assembled TBSV particles. TBSV–wt and all the TBSV–chimeras VNPs were probed separately with specific anti-tag antibodies. A total soluble protein extract from a not-infected (NI) *N. benthamiana* plant was used as a negative control

presence of the peptides at protein level, their exposure on virion surface and the accessibility for antibodies binding.

Access to the internal cavity of VNPs

In general two main strategies have been adopted to load a cargo inside VNPs: (1) in vitro assembly of the VNPs (Chen et al. 2006; Comellas-Aragones et al. 2007; Ren et al. 2006) and (2) reversal viral pore gating (Douglas and Young 1998; Loo et al. 2006), both achieved in presence of high concentration of the exogenous molecules.

In the case of the TBSV, the inner core can be reached by switchable pH dependent gating (Aramayo et al. 2005; Kruse et al. 1982). Many aspects of virus assembly were addressed and physicochemical conditions for the reversible opening of gated pores were defined. We applied slightly alkaline conditions and divalent ion chelators to promote conformational changes necessary for particle loading. As proof of concept, the loading of the small EtBr molecule into swollen TBSV nanoparticles was tested.

Approximately 4 µg of purified TBSV–wt or –Flag particles were incubated at 4 °C for 2 h in swelling buffer (0.1 M Tris, 50 mM EDTA, pH 8.5; Fig. 5a, lanes 2, 4) or control buffer (0.1 M Tris, pH 5.5; Fig. 5a, lanes 1, 3), both containing EtBr (0.5 µg/ml). The samples were then resolved by agarose gel electrophoresis and visualized under UV light. According to the nature of the EtBr molecule, the signal was visible only when this compound penetrated into cavity of swollen particles intercalating the viral RNA (Fig. 5a, upper panel, lanes 2, 4). Therefore, fluorescence was not detectable in lanes containing the virions being in compact state (Fig. 5a, upper panel, lanes 1, 3). When the whole gel, after the run, was incubated in swelling buffer and fresh EtBr was added, the particles previously in compact state underwent swelling and became visible once exposed to UV light (Fig. 5a, middle panel, lanes 1, 3). The assembly of the TBSV based nanoparticles after the treatments has been proved by staining the same gel with Coomassie Brilliant Blue, highlighting the co-migration of genomic RNA with capsid proteins (Fig. 5a, lower panel). To further test cations depletion and alkaline conditions as prerequisites for the accessibility to the viral RNA contained in the VNPs' cavity, TBSV–wt or –Flag particles were challenged for susceptibility to RNAse activity in both control and swelling buffer (Fig. 5b). RNA nuclease processing was

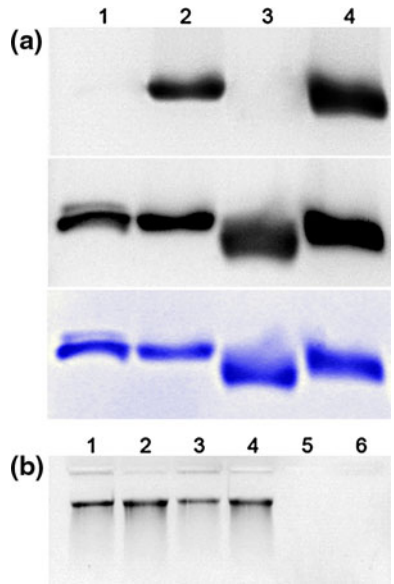

Fig. 5 Evaluation of TBSV internal cavity accessibility. **a** EtBr loading by controlled TBSV capsid expansion. *Upper panel* agarose gel of TBSV–wt (*lanes 1*, *2*) and TBSV–Flag particles (*lanes 3*, *4*) incubated with EtBr in swollen (*lanes 2*, *4*) or compact state (*lanes 1*, *3*). Further, the same gel was incubated in swelling buffer supplemented with EtBr (*middle panel*) and then stained with Coomassie Blue (*lower panel*). **b** Ribonuclease A protection assay. Agarose gel electrophoresis of TBSV extracted RNAs. Untreated TBSV particles were used as control of genome extraction (*lane 1* TBSV–wt, and *2* TBSV–Flag). Purified particles were treated with ribonuclease A in compact (*lane 3* TBSV–wt, and *lane 4* TBSV–Flag) or swollen state (*lane 5*, TBSV–wt, and *lane 6*, TBSV–Flag) before RNA extraction

investigated to evaluate digestion: viral genomic RNA was extracted from VNPs used in each treatment and analyzed by agarose gel electrophoresis. The RNA enclosed in the TBSV nanoparticles at pH 8.5 supplemented with EDTA 50 mM was completely degraded (Fig. 5b, lanes 5, 6) whereas the genome within virions at pH 5.5 resulted fully protected (Fig. 5b, lanes 3, 4), as the untreated particles' controls (Fig. 5b, lanes 1, 2).

Chemical derivatization of VNPs

Bioconjugation of biotin by NHS ester based chemistry was tested to investigate the capability of TBSV nanoparticles to be addressed by chemical derivatization. NHS–PEO_4 biotin (Pierce) reacts with primary amines creating a stable amide bond through NHS ester. Although the TBSV CP contains 13 lysine residues in its primary structure, it has been shown that, in the arrangement of the quaternary structure of the properly assembled virion, primary amines contained in their side chain are not accessible (Harrison et al. 1978; Olson et al. 1983). As previously described, the required lysine residues were indeed introduced, by genetic modification, on the outer surface of each of the chimeric TBSV nanoparticles through the Flag tag fusion (DYKDDDDK) which is ubiquitously present on each CVNPs as last heterologous portion at the C-terminus of the chimeric CPs (see Fig. 1 for the related c-DNA constructs).

TBSV–wt or –Flag nanoparticles were incubated with a tenfold molar excess of NHS–PEO_4–Biotin for 24 h. The non-reacted biotin reagent and the byproducts of the reaction (the NHS leaving group) were then removed by chromatography during the desalting step on a spin column. A sample from each purified reaction was analyzed by ELISA and western blot using a HRP-conjugated streptavidin as a probe (Online Resource 2a, b, lower panel). The results confirmed that TBSV–wt is unsuitable for conjugation to biotin by NHS ester based chemistry (Online Resource 2b, lower panel, lanes 1, 2). In contrast, the presence of biotin-nanoparticles conjugates was successfully confirmed for TBSV–Flag particles (Online Resource 2b, lower panel, lanes 3, 4). The presence of TBSV CPs was additionally detected through a silver stained SDS–PAGE (Online Resource 2b, upper panel).

Infections by in planta transcription of cDNA based constructs

An alternative in vivo transcription model based on plant expression strategy was designed. Three constructs have been assembled: 35S–TBSV–cMyc, –cMyc.NOS and –cMyc.riboNOS (Fig. 1h–j). To test the infectivity of the 3 different expression vectors, 5 plants of *N. benthamiana* were inoculated on 2 leaves per plant with each of the different purified cDNA expression constructs at 3 different concentrations: 10, 20 or 30 μg. The symptomatology was constantly monitored and documented by photo capturing. Using 10 μg of plasmid none of the vectors was able to establish the infection. With 20 μg, at 10 dpi only upper leaves of plants inoculated with 35S–TBSV–cMyc.riboNOS vector showed evident systemic viral symptoms. With 30 μg the 35S–TBSV–cMyc.riboNOS vector produced systemic symptoms at already 6–8 dpi, whereas the 35S–TBSV–cMyc.NOS showed

some mild signs of infection only at 19 dpi. All the attempts performed with linearized 35S–TBSV–cMyc vector, used at 3 different concentrations for inoculation, failed to induce both local symptoms development and systemic virus spread.

As final biological prove of infection a cycle of re-inoculations was performed using the sap obtained homogenizing the symptomatic systemic tissue of all infected plants. All primary infections were confirmed.

The use of 30 μg of the 35S–TBSV–cMyc.ribo-NOS type of vector showed to be so efficient that it could be employed routinely to establish primary infections for production purposes, thus avoiding the in vitro transcription step.

Discussion

Nanotechnology's need for defined, repetitive and nanoscale structures can find in VNPs an almost inextinguishable source of buildingblocks, scaffolds and particulate arrangements. It is estimated that viruses are the second most prevalent biological entity on the planet (Suttle 2005). Many different viruses of the most diverse origin have been studied for their potential use as structured bioinspired nanomaterials and nanodevices (Grasso and Santi 2010). Plant virus based systems are among the most advanced and exploited. More than 800 plant virus genomes are completely sequenced (data retrieved from viruses complete genomes at NCBI database: http://www.ncbi.nlm.nih.gov), the majority having a small single stranded positive RNA nature. Increasing knowledge on virus structure, genetics, replication, host range and fitness has already allowed the development of well established platforms (Gopinath et al. 2000; Kumagai et al. 1993; Lico et al. 2006; Liu et al. 2005; Yildiz et al. 2012; Ziegler et al. 2000).

In this light, the TBSV pepper isolate infectious cDNA clone was used for genetic engineering. Construct design strategy was developed to address the sequential insertion of 4 peptide modules to test the ability of the system to accommodate increasingly longer sequences. The choice of employing the well known and commonly used FLAG, cMyc, HA and V5 tags was made for the availability of commercial reagents and protocols. A sequence coding for a GGPGGGG linker peptide, spacing the CP and the heterologous portion, was designed in all constructs. This sequence was employed primarily for the well documented ability of GPG to interrupt protein secondary structures, providing flexibility to the residing region and, consequently, promoting each peptide to assume its original conformation independently of other modules (Wriggers et al. 2005). For these reasons, sequences were designed to have also GPG linkers between each module. FLAG was the first peptide introduced and it is therefore present at the C-terminal end of each CVNP (Fig. 1d–g). Its octapeptide sequence (DYKDDDDK) contains lysine and aspartic acid residues that, together with cysteines, are the most commonly addressed amino acids for chemical derivatization of VNPs (Steinmetz et al. 2010).

Nicotiana benthamiana plants are excellent bioreactors for supporting VNPs production in both laboratory setting and large scale production facilities. These plants are easy to grow and handle, being required only 8 weeks from seeds to the proper developmental stage for infection. Moreover, *N. benthamiana* plants are neither food nor feed and their use for production of plant made recombinant pharmaceuticals is so diffused that can almost be considered a standard (Goodin et al. 2008; Lico et al. 2008; Twyman 2005; Twyman 2008; Webster et al. 2009). Mechanical leaf rubbing inoculation was performed to test the different constructs. Simptomatology and kinetics of infection were very homogeneous among different chimeras. Production time can be estimated in just 10 days from tissue inoculation to purified VNPs. Chimeras were able to self assemble in vivo as demonstrated by comparing, on a sucrose gradient, each sedimentation profile to TBSV–wt (Fig. 2b). Direct prove of assembly was also verified by electron microscopy, that allowed to unequivocally demonstrate CVNPs homogeneity regarding both dimensions and shape (Fig. 3). The purification procedure is reliable, efficient and clean. The system consistently allows to produce approximately 300 mg of purified VNPs per kg of fresh infected leaves. Data collected from several independent experiments suggest that VNPs yield after purification was very similar among different CVNPs.

Plant material deriving from inoculated and systemically infected leaves was used to characterize the different CVNPs at protein level and to evaluate vector stability at nucleic acid level. ELISA was employed to test the reactivity of plant crude extracts, using the different anti-tags antibodies available. Data not only

confirmed the expected display of each exogenous peptide module, but also revealed that the progressive fusion of different peptides did not affect the structure required for their molecular recognition. In fact, in the multi-modules assemblies (TBSV–cMyc, –HA and –V5) each tag was efficiently recognized when individually probed with the respective antibody (Fig. 4c). In general terms, independent structural folding would be particularly precious when using multiple display assembly of antigens for vaccine development, which is the oldest and one of most promising applications of plant based VNPs in biomedicine (Chen and Lai 2013; Lico et al. 2009; Lico et al. 2012; Montague et al. 2011; Steinmetz et al. 2009; Tyulkina et al. 2011). In addition, this feature could be effectively employed in targeted delivery of VNPs for displaying more than one moiety on the particle surface (Work et al. 2004). Correct fusion protein expression was also confirmed on purified CVNPs by western blot analysis, using the anti-Flag antibody. The mobility shift among the chimeric and wild-type CPs was clearly related to the respective sizes (Fig. 4b).

We were successfully able to display up to 56 additional amino acids as C-terminal fusion (TBSV–V5). Regardless from the attempt of displaying the entire GFP (238 aa), which resulted in a non-infectious construct (data not shown), TBSV–V5 was the longest assembly we tested, leaving the door open to even longer fusions. In any case it has to be stressed that length is not the only parameter to consider: charge, shape, dimension and affinity are all fundamental features, which mostly rely on the chemical nature of the fused heterologous sequence. Hence, each new chimera must be evaluated empirically on a case to case basis.

Construct instability has been reported in different systems. In fact, sometimes the added sequence can impair viral fitness, thus viral genome can rearrange with single or multiple mutations to acquire more stability. It is also possible a complete recombinational event with the total extrusion of the heterologous portion to reset viral genome to the initial wild-type configuration (Avesani et al. 2007; Haviv et al. 2006; Lico et al. 2006). Integrity of the sequence at nucleic acid level was here evaluated by RT-PCR and fragments sequencing (Fig. 4a). Recombination of chimeric replicons, isolated from inoculated and systemic leaves of first and second generation infections, has never been detected. Beyond second generation we have sporadically experienced some construct instability, especially when the largest fusions were concerned (data not shown). In this regard, we have found very convenient to use in vitro transcribed RNA directly for production purposes and we believe that it is indeed feasible to use just first generation material for small scale production. Under this view and with the prospect of a scaled up process, we designed and assembled an in planta expression cDNA based construct, that could be delivered to plants simply in the form of a circular DNA plasmid under the control of sequences active in plants, therefore avoiding the enzymatic treatment necessary for the in vitro transcription. Consequently, a high copy plasmid was used as backbone to support the assembly of a plant expression construct containing: the CaMV 35S promoter, the infectious viral cDNA, the HRz sequence and the NOS terminator (35S–TBSV–cMyc.riboNOS, Fig. 1j). Upon mechanical leaf rubbing inoculation we demonstrated that 30 μg of this vector are able to reproducibly establish infections comparable, in regards of symptomatology and progression, to the one generated by in vitro transcribed RNAs. The employment of HRz sequence, previously reported for TBSV (Scholthof 1999), promotes an autocatalytic process at RNA level that results, upon cleavage of the acquired poly (A) tail, in the generation of the correct viral 3′ end, essential for an efficient replication (Chowrira et al. 1994).

In vitro chemical modification of VNPs relies on the covalent binding of an activated conjugate to functional groups of amino acids residues of the virus structural proteins. The amine functional group of lysine is a common target for conjugation through NHS ester based chemistry (Smith et al. 2006; Wang et al. 2002). Thirteen lysine residues are part of the 388 amino acids long TBSV CP (pepper isolate) (Szittya et al. 2000), 8 of which reside in the internal R domain, 5 in the S domain and none in the protruding P domain. Therefore no primary amines are exposed and addressable on the outer viral shell (Hsu et al. 2006). Nevertheless, Flag (DYKDDDDK), which is the most distal peptide on each chimera, carries 2 lysine residues, one as the very last carboxi-terminus. Biotin NHS esters were used to probe for reactive amine groups exposed on Flag CVNPs. Although the number of addressed lysine residues has not been evaluated and it will be the object of future studies, effective biotinylation of Flag CVNPs was proved using

streptavidin probes in both western blot and ELISA (Online Resource 2a and 2b, lower panel). Conversely, as predicted, it was not possible to functionalize unmodified wild-type virions.

Chemical derivatization of lysine functional groups has been exploited using other plant derived VNPs systems such as the case of successfully displaying fluorescent dyes for in vivo imaging (Lewis et al. 2006) and folic acid for cancer cells specific targeting (Ren et al. 2007). Moreover, bioconjugation of biotin on plant VNPs has been used to employ the strong non-covalent bond between biotin and streptavidin. In essence this interaction can be used to redecorate VNPs surface with proteins of interest fused to streptavidin. By uncoupling the expression of the VNP scaffold and of the protein to expose, very large assemblies, otherwise very difficult to generate, have been achieved (Smith et al. 2006).

The employment of other native or genetically introduced amino acid functional groups, such as carboxylates from aspartic and glutamic acids, thiol from cysteine, and tyrosine together with a more quantitative characterization and optimization of conjugation's conditions will greatly expand the range of different chemistries, and their combinations, for addressing VNPs.

Viral capsids play different roles according to the influence of the surrounding molecular environment. Protection, delivery and discharge of their genetic cargo are fundamental functions for virus propagation. Many aspects of structural transition sustaining these viral functions have been addressed using a variety of biochemical and biophysical techniques setting the conceptual ground for using these objects as nanocontainers (Johnson and Chiu 2000; Ma et al. 2012; Yildiz et al. 2011). Although the interior plant virus cavity has not been addressed as much the external surface, several studies exploited specific viral structural properties to gain access to VNPs' inner core. Some plant viruses efficiently assemble into mature capsids in vitro. The process of disassembly/reassembly can be promoted by providing the proper physicochemical conditions. Consequently, cargo entrapment can be established by capsid reassembly in presence of high concentration of the exogenous molecules (Loo et al. 2006; Ren et al. 2006). On the other hand, the inner side of icosahedral viruses, such as TBSV, can be reached by reversible opening of virion gated pores. In fact, it has been demonstrated that many of these structures, at the interface of their capsomeric subunits, carry divalent cations, typically Ca^{2+} (Speir et al. 1995) but also Mg^{2+} (Lucas et al. 2002), which appear to be essential for virion structural stability. In particular, the TBSV swelling process has been widely studied by different approaches which revealed that its inner core can be reached by switchable pH and divalent ion-dependent gating (Aramayo et al. 2005). In fact, by depletion of divalent cations (using EDTA 50 mM) in slightly alkaline conditions (pH 8.5) at 4 °C for 2 h we were able to address the interior cavity of TBSV particles setting the ground for cargo loading. We first demonstrated that genomic RNAs, contained inside VNPs in relaxed (swollen) state, were accessible to RNAase, while genomes contained in VNPs in compact state were inaccessible and therefore protected from degradation (Fig. 5b). Moreover, switching between the two conformational states, we were able to load EtBr inside the VNPs as clearly revealed by the fluorescence emission derived from the intercalation of this fluorophore into the nucleic acids contained inside the viral cavity (Fig. 5a). We decided to use EtBr mainly for analytical reasons in order to provide a proof of concept in the prospect of loading TBSV core with chemical molecules of pharmacological activity. In fact, EtBr has a size and chemical nature in the range of many drugs and it is currently used in veterinary medicine to treat trypanosomosis in cattle (Stevenson et al. 1995).

In conclusion, in this study we have presented the development and characterization of a TBSV based nanovector that can be used for the encapsulation of small molecules and on which a predictable and programmable genetic and/or chemical engineering can be performed. Safety, production efficiency, industrial scalability and versatility related to possible modifications are peculiar strengths of this system. Modification by design of novel VNPs properties, together with the possibility of generating organized arrays using VNPs as nanoblock components, have the potential to create multifunctional structures able to diagnose diseases, deliver therapeutic agents, monitor treatment progression, support catalytic reactions and sustain in vitro cell proliferation and differentiation. However, any new functionality must be carefully evaluated in regard of the VNPs properties and fate. More detailed studies concerning the in vivo behavior of VNPs in terms of biocompatibility, bioavailability, biodistribution, pharmacokinetics, immunogenicity and toxicity are of paramount importance so that this technology will be able to live up to its potential.

Acknowledgments We thank Dr. Jozsef Burgyan and Dr. Gyorgy Szittya for the original infectious TBSV–P cDNA clone and Dr. Anna Rita Taddei for technical assistance regarding the electron microscopy visualizations of TBSV derived particles.

References

Aramayo R, Merigoux C, Larquet E, Bron P, Perez J, Dumas C, Vachette P, Boisset N (2005) Divalent ion-dependent swelling of tomato bushy stunt virus: a multi-approach study. Biochim Biophys Acta 1724(3):345–354. doi:10.1016/j.bbagen.2005.05.020

Ashley CE, Carnes EC, Phillips GK, Durfee PN, Buley MD, Lino CA, Padilla DP, Phillips B, Carter MB, Willman CL, Brinker CJ, Caldeira CJ, Chackerian B, Wharton W, Peabody DS (2011) Cell-specific delivery of diverse cargos by bacteriophage MS2 virus-like particles. ACS Nano 5(7):5729–5745. doi:10.1021/nn201397z

Avesani L, Marconi G, Morandini F, Albertini E, Bruschetta M, Bortesi L, Pezzotti M, Porceddu A (2007) Stability of *Potato virus* X expression vectors is related to insert size: implications for replication models and risk assessment. Transgenic Res 16(5):587–597. doi:10.1007/s11248-006-9051-1

Bar H, Yacoby I, Benhar I (2008) Killing cancer cells by targeted drug-carrying phage nanomedicines. BMC Biotechnol 8:37. doi:10.1186/1472-6750-8-37

Baulcombe DC, Chapman S, Santa Cruz S (1995) Jellyfish green fluorescent protein as a reporter for virus infections. Plant J 7(6):1045–1053

Beterams G, Bottcher B, Nassal M (2000) Packaging of up to 240 subunits of a 17 kDa nuclease into the interior of recombinant hepatitis B virus capsids. FEBS Lett 481(2):169–176

Burgyan J, Russo M (1998) Tombusvirus isolation and RNA extraction. Methods Mol Biol 81:225–230. doi:10.1385/0-89603-385-6:225

Chen Q, Lai H (2013) Plant-derived virus-like particles as vaccines. Hum Vaccines 9(1). doi:10.4161/hv.22218

Chen C, Daniel MC, Quinkert ZT, De M, Stein B, Bowman VD, Chipman PR, Rotello VM, Kao CC, Dragnea B (2006) Nanoparticle-templated assembly of viral protein cages. Nano Lett 6(4):611–615. doi:10.1021/nl0600878

Chiang CM, Roeder RG (1993) Expression and purification of general transcription factors by FLAG epitope-tagging and peptide elution. Pept Res 6(2):62–64

Chowrira BM, Pavco PA, McSwiggen JA (1994) In vitro and in vivo comparison of hammerhead, hairpin, and hepatitis delta virus self-processing ribozyme cassettes. J Biol Chem 269(41):25856–25864

Comellas-Aragones M, Engelkamp H, Claessen VI, Sommerdijk NA, Rowan AE, Christianen PC, Maan JC, Verduin BJ, Cornelissen JJ, Nolte RJ (2007) A virus-based single-enzyme nanoreactor. Nat Nanotechnol 2(10):635–639. doi:10.1038/nnano.2007.299

Depicker A, Stachel S, Dhaese P, Zambryski P, Goodman HM (1982) Nopaline synthase: transcript mapping and DNA sequence. J Mol Appl Genet 1(6):561–573

Douglas T, Young M (1998) Host-guest encapsulation of materials by assembled virus protein cages. Nature 393(6681):152–155

Fowler CE, Shenton W, Stubbs G, Mann S (2001) Tobacco mosaic virus liquid crystals as templates for the interior design of silica mesophases and nanoparticles. Adv Mater 13:1266–1269

Gleiter S, Lilie H (2001) Coupling of antibodies via protein Z on modified polyoma virus-like particles. Protein Sci 10(2):434–444. doi:10.1110/ps.31101

Gonzalez MJ, Plummer EM, Rae CS, Manchester M (2009) Interaction of Cowpea mosaic virus (CPMV) nanoparticles with antigen presenting cells in vitro and in vivo. PLoS One 4(11):e7981. doi:10.1371/journal.pone.0007981

Goodin MM, Zaitlin D, Naidu RA, Lommel SA (2008) Nicotiana benthamiana: its history and future as a model for plant–pathogen interactions. Mol Plant Microbe Interact 21(8):1015–1026. doi:10.1094/MPMI-21-8-1015

Gopinath K, Wellink J, Porta C, Taylor KM, Lomonossoff GP, van Kammen A (2000) Engineering cowpea mosaic virus RNA-2 into a vector to express heterologous proteins in plants. Virology 267(2):159–173. doi:10.1006/viro.1999.0126

Grasso S, Santi L (2010) Viral nanoparticles as macromolecular devices for new therapeutic and pharmaceutical approaches. Int J Physiol Pathophysiol Pharmacol 2(2):161–178

Hajitou A, Trepel M, Lilley CE, Soghomonyan S, Alauddin MM, Marini FCR, Restel BH, Ozawa MG, Moya CA, Rangel R, Sun Y, Zaoui K, Schmidt M, von Kalle C, Weitzman MD, Gelovani JG, Pasqualini R, Arap W (2006) A hybrid vector for ligand-directed tumor targeting and molecular imaging. Cell 125(2):385–398. doi:10.1016/j.cell.2006.02.042

Harrison SC, Olson AJ, Schutt CE, Winkler FK, Bricogne G (1978) Tomato bushy stunt virus at 2.9 Å resolution. Nature 276(5686):368–373

Haviv S, Galiakparov N, Goszczynski DE, Batuman O, Czosnek H, Mawassi M (2006) Engineering the genome of *Grapevine virus* A into a vector for expression of proteins in herbaceous plants. J Virol Methods 132(1–2):227–231. doi:10.1016/j.jviromet.2005.10.020

Hearne PQ, Knorr DA, Hillman BI, Morris TJ (1990) The complete genome structure and synthesis of infectious RNA from clones of tomato bushy stunt virus. Virology 177(1):141–151

Hsu C, Singh P, Ochoa W, Manayani DJ, Manchester M, Schneemann A, Reddy VS (2006) Characterization of polymorphism displayed by the coat protein mutants of tomato bushy stunt virus. Virology 349(1):222–229. doi:10.1016/j.virol.2006.02.038

Johnson JE, Chiu W (2000) Structures of virus and virus-like particles. Curr Opin Struct Biol 10(2):229–235

Kawarasaki Y, Yamada Y, Ichimori M, Shinbata T, Kohda K, Nakano H, Yamane T (2003) Stabilization of affinity-tagged recombinant protein during/after its production in a cell-free system using wheat-germ extract. J Biosci Bioeng 95(3):209–214

Kolodziej KE, Pourfarzad F, de Boer E, Krpic S, Grosveld F, Strouboulis J (2009) Optimal use of tandem biotin and V5 tags in ChIP assays. BMC Mol Biol 10:6. doi:10.1186/1471-2199-10-6

Kruse J, Kruse KM, Witz J, Chauvin C, Jacrot B, Tardieu A (1982) Divalent ion-dependent reversible swelling of tomato bushy stunt virus and organization of the expanded virion. J Mol Biol 162(2):393–414. doi:0022-2836(82)90534-4

Kumagai MH, Turpen TH, Weinzettl N, Della-Cioppa G, Turpen AM, Donson J, Hilf ME, Grantham GL, Dawson WO, Chow TP et al (1993) Rapid, high-level expression of biologically active alpha-trichosanthin in transfected plants by an RNA viral vector. Proc Natl Acad Sci USA 90(2):427–430

Laemmli UK (1970) Cleavage of structural proteins during the assembly of the head of bacteriophage T4. Nature 227(5259):680–685

Lai H, Chen Q (2012) Bioprocessing of plant-derived virus-like particles of Norwalk virus capsid protein under current good manufacture practice regulations. Plant Cell Rep 31(3):573–584

Laize V, Ripoche P, Tacnet F (1997) Purification and functional reconstitution of the human CHIP28 water channel expressed in Saccharomyces cerevisiae. Protein Expr Purif 11(3):284–288. doi:10.1006/prep.1997.0798

Lewis JD, Destito G, Zijlstra A, Gonzalez MJ, Quigley JP, Manchester M, Stuhlmann H (2006) Viral nanoparticles as tools for intravital vascular imaging. Nat Med 12(3): 354–360. doi:10.1038/nm1368

Lico C, Capuano F, Renzone G, Donini M, Marusic C, Scaloni A, Benvenuto E, Baschieri S (2006) Peptide display on *Potato virus* X: molecular features of the coat protein-fused peptide affecting cell-to-cell and phloem movement of chimeric virus particles. J Gen Virol 87(Pt 10):3103–3112. doi:10.1099/vir.0.82097-0

Lico C, Chen Q, Santi L (2008) Viral vectors for production of recombinant proteins in plants. J Cell Physiol 216(2):366–377. doi:10.1002/jcp.21423

Lico C, Mancini C, Italiani P, Betti C, Boraschi D, Benvenuto E, Baschieri S (2009) Plant-produced *Potato virus* X chimeric particles displaying an influenza virus-derived peptide activate specific CD8+ T cells in mice. Vaccine 27(37): 5069–5076. doi:10.1016/j.vaccine.2009.06.045

Lico C, Santi L, Twyman RM, Pezzotti M, Avesani L (2012) The use of plants for the production of therapeutic human peptides. Plant Cell Rep 31(3):439–451. doi:10.1007/s00299-011-1215-7

Liu L, Canizares MC, Monger W, Perrin Y, Tsakiris E, Porta C, Shariat N, Nicholson L, Lomonossoff GP (2005) Cowpea mosaic virus-based systems for the production of antigens and antibodies in plants. Vaccine 23(15):1788–1792. doi: 10.1016/j.vaccine.2004.11.006

Loo L, Guenther RH, Basnayake VR, Lommel SA, Franzen S (2006) Controlled encapsidation of gold nanoparticles by a viral protein shell. J Am Chem Soc 128(14):4502–4503. doi:10.1021/ja057332u

Loo L, Guenther RH, Lommel SA, Franzen S (2008) Infusion of dye molecules into red clover necrotic mosaic virus. Chem Commun (Camb) 1:88–90

Lucas RW, Larson SB, McPherson A (2002) The crystallographic structure of brome mosaic virus. J Mol Biol 317(1):95–108. doi:10.1006/jmbi.2001.5389

Ma Y, Nolte RJ, Cornelissen JJ (2012) Virus-based nanocarriers for drug delivery. Adv Drug Deliv Rev 64(9):811–825. doi: 10.1016/j.addr.2012.01.005

McCormick AA, Corbo TA, Wykoff-Clary S, Nguyen LV, Smith ML, Palmer KE, Pogue GP (2006) TMV-peptide fusion vaccines induce cell-mediated immune responses and tumor protection in two murine models. Vaccine 24(40–41):6414–6423. doi:10.1016/j.vaccine.2006.06.003

Montague NP, Thuenemann EC, Saxena P, Saunders K, Lenzi P, Lomonossoff GP (2011) Recent advances of cowpea mosaic virus-based particle technology. Hum Vaccin 7(3):383–390. doi:14989

Murata Y, Lightfoote PM, Rose RC, Walsh EE (2009) Antigenic presentation of heterologous epitopes engineered into the outer surface-exposed helix 4 loop region of human papillomavirus L1 capsomeres. Virol J 6:81. doi:10.1186/1743-422X-6-81

Nam KT, Kim DW, Yoo PJ, Chiang CY, Meethong N, Hammond PT, Chiang YM, Belcher AM (2006) Virus-enabled synthesis and assembly of nanowires for lithium ion battery electrodes. Science 312(5775):885–888. doi:10.1126/science.1122716

Newton-Northup JR, Figueroa SD, Quinn TP, Deutscher SL (2009) Bifunctional phage-based pretargeted imaging of human prostate carcinoma. Nucl Med Biol 36(7):789–800. doi:10.1016/j.nucmedbio.2009.04.010

Odell JT, Nagy F, Chua NH (1985) Identification of DNA sequences required for activity of the cauliflower mosaic virus 35S promoter. Nature 313(6005):810–812

Olson AJ, Bricogne G, Harrison SC (1983) Structure of tomato bushy stunt virus IV. The virus particle at 2.9 Å resolution. J Mol Biol 171(1):61–93

Prasuhn DE Jr, Yeh RM, Obenaus A, Manchester M, Finn MG (2007) Viral MRI contrast agents: coordination of Gd by native virions and attachment of Gd complexes by azide-alkyne cycloaddition. Chem Commun (Camb) 12:1269–1271. doi:10.1039/b615084e

Raja KS, Wang Q, Gonzalez MJ, Manchester M, Johnson JE, Finn MG (2003) Hybrid virus-polymer materials. 1. Synthesis and properties of PEG-decorated cowpea mosaic virus. Biomacromolecules 4(3):472–476. doi:10.1021/bm025740

Ren Y, Wong SM, Lim LY (2006) In vitro-reassembled plant virus-like particles for loading of polyacids. J Gen Virol 87(Pt 9):2749–2754. doi:10.1099/vir.0.81944-0

Ren Y, Wong SM, Lim LY (2007) Folic acid-conjugated protein cages of a plant virus: a novel delivery platform for doxorubicin. Bioconjug Chem 18(3):836–843. doi:10.1021/bc060361p

Sambrook J, Russell DW (2001) Molecular cloning: a laboratory manual. Cold Spring Harbor Laboratory Press, Cold Spring Harbor

Santi L, Huang Z, Mason H (2006) Virus-like particles production in green plants. Methods 40(1):66–76. doi:10.1016/j.ymeth.2006.05.020

Santi L, Batchelor L, Huang Z, Hjelm B, Kilbourne J, Arntzen CJ, Chen Q, Mason HS (2008) An efficient plant viral expression system generating orally immunogenic Norwalk virus-like particles. Vaccine 26(15):1846–1854. doi: 10.1016/j.vaccine.2008.01.053

Scholthof HB (1999) Rapid delivery of foreign genes into plants by direct rub-inoculation with intact plasmid DNA of a tomato bushy stunt virus gene vector. J Virol 73(9):7823–7829

Scholthof HB, Scholthof KB, Jackson AO (1996) Plant virus gene vectors for transient expression of foreign proteins in plants. Annu Rev Phytopathol 34:299–323. doi:10.1146/annurev.phyto.34.1.299

Singh P (2009) Tumor targeting using canine parvovirus nanoparticles. Curr Top Microbiol Immunol 327:123–141

Smith ML, Lindbo JA, Dillard-Telm S, Brosio PM, Lasnik AB, McCormick AA, Nguyen LV, Palmer KE (2006) Modified tobacco mosaic virus particles as scaffolds for display of protein antigens for vaccine applications. Virology 348(2):475–488. doi:10.1016/j.virol.2005.12.039

Speir JA, Munshi S, Wang G, Baker TS, Johnson JE (1995) Structures of the native and swollen forms of cowpea chlorotic mottle virus determined by X-ray crystallography and cryo-electron microscopy. Structure 3(1):63–78

Steinmetz NF, Lin T, Lomonossoff GP, Johnson JE (2009) Structure-based engineering of an icosahedral virus for nanomedicine and nanotechnology. Curr Top Microbiol Immunol 327:23–58

Steinmetz NF, Mertens ME, Taurog RE, Johnson JE, Commandeur U, Fischer R, Manchester M (2010) *Potato virus* X as a novel platform for potential biomedical applications. Nano Lett 10(1):305–312. doi:10.1021/nl9035753

Stevenson P, Sones KR, Gicheru MM, Mwangi EK (1995) Comparison of isometamidium chloride and homidium bromide as prophylactic drugs for trypanosomiasis in cattle at Nguruman, Kenya. Acta Trop 59(2):77–84. doi:0001-706X(94)00080-K

Strable E, Johnson JE, Finn MG (2004) Natural nanochemical building blocks: icosahedral virus particles organized by attached oligonucleotides. Nano Lett 4(8):1385–1389. doi:10.1021/nl0493850

Suttle CA (2005) Viruses in the sea. Nature 437(7057):356–361. doi:10.1038/nature04160

Szittya G, Salamon P, Burgyan J (2000) The complete nucleotide sequence and synthesis of infectious RNA of genomic and defective interfering RNAs of TBSV–P. Virus Res 69(2):131–136

Twyman RM (2005) Host plants systems and expression strategies for molecular farming? In: Fischer R, Schillberg S (eds) Molecular farming: plant-made pharmaceuticals and technical proteins. Wiley-VCH Verlag GmbH & Co., KGaA, UK, pp 191–216

Twyman RM (2008) Large-scale protein production in plants: host plants, systems and expression. In: Fersht AR (ed) Protein science encyclopedia. Wiley, UK

Tyulkina LG, Skurat EV, Frolova OY, Komarova TV, Karger EM, Atabekov IG (2011) New viral vector for superproduction of epitopes of vaccine proteins in plants. Acta Naturae 3(4):73–82

van Houten NE, Zwick MB, Menendez A, Scott JK (2006) Filamentous phage as an immunogenic carrier to elicit focused antibody responses against a synthetic peptide. Vaccine 24(19):4188–4200. doi:10.1016/j.vaccine.2006.01.001

Wang Q, Kaltgrad E, Lin T, Johnson JE, Finn MG (2002) Natural supramolecular building blocks. Wild-type cowpea mosaic virus. Chem Biol 9(7):805–811

Webster DE, Wang L, Mulcair M, Ma C, Santi L, Mason HS, Wesselingh SL, Coppel RL (2009) Production and characterization of an orally immunogenic *Plasmodium antigen* in plants using a virus-based expression system. Plant Biotechnol J 7(9):846–855. doi:10.1111/j.1467-7652.2009.00447.x

White KA, Nagy PD (2004) Advances in the molecular biology of tombusviruses: gene expression, genome replication, and recombination. Prog Nucleic Acid Res Mol Biol 78:187–226. doi:10.1016/S0079-6603(04)78005-8

Work LM, Ritchie N, Nicklin SA, Reynolds PN, Baker AH (2004) Dual targeting of gene delivery by genetic modification of adenovirus serotype 5 fibers and cell-selective transcriptional control. Gene Ther 11(16):1296–1300. doi:10.1038/sj.gt.33022923302292

Wriggers W, Chakravarty S, Jennings PA (2005) Control of protein functional dynamics by peptide linkers. Biopolymers 80(6):736–746. doi:10.1002/bip.20291

Yildiz I, Shukla S, Steinmetz NF (2011) Applications of viral nanoparticles in medicine. Curr Opin Biotechnol 22(6):901–908. doi:10.1016/j.copbio.2011.04.020

Yildiz I, Tsvetkova I, Wen AM, Shukla S, Masarapu MH, Dragnea B, Steinmetz NF (2012) Engineering of Brome mosaic virus for biomedical applications. RSC Adv 2:3670–3677. doi:10.1039/C2RA01376B

Ziegler A, Cowan GH, Torrance L, Ross HA, Davies HV (2000) Facile assessment of cDNA constructs for expression of functional antibodies in plants using the *Potato virus* X vector. Mol Breed 6:327–335